IOP PUBLISHING JOURNAL OF PHYSICS D: APPLIED PHYSICS

J. Phys. D: Appl. Phys. **43** (2010) 215102 (7pp) doi:10.1088/0022-3727/43/21/215102

# Influence of temperature and illumination on the electrical properties of p-ZnTe/n-CdTe heterojunction grown by molecular beam epitaxy

**A A M Farag[1], I S Yahia[1,3], T Wojtowicz[2] and G Karczewski[2]**

[1] Physics Department, Faculty of Education, Ain Shams University, Roxy, Cairo, Egypt
[2] Institute of Physics, Polish Academy of Sciences, Al. Lotników, 32/46, 02-668 Warszawa, Poland

E-mail: dr_isyahia@yahoo.com and isyahia@gmail.com

Received 2 December 2009, in final form 23 April 2010
Published 13 May 2010
Online at stacks.iop.org/JPhysD/43/215102

**Abstract**

A set of p-ZnTe/n-CdTe heterojunctions were grown on conducting GaAs substrates by molecular beam epitaxy. The current density–voltage ($J$–$V$) and capacitance–voltage ($C$–$V$) characteristics measured in the temperature range 300–400 K were analysed in order to reveal the dominant carrier transport mechanisms through the junctions. The $C$–$V$ measurements show that the device is linearly graded. The temperature dependence of the built-in potential and the impurity gradient of the device were determined. The deep defect states govern the current flow through the junctions. The measurements under the lower voltage region ($V < 0.35$ V) reveal at the p-ZnTe/n-CdTe interface, the presence of deep defect states with the activation energy of 0.52 eV. Under the higher forward bias voltage ($V > 0.35$ V), the space-charge-limited current governed the $J$–$V$ characteristics with a single traps level, $\Delta E_t = 0.55$ eV. The p-ZnTe/n-CdTe device under different illumination intensities exhibit a significant photosensitivity proving that this kind of heterostructure can be regarded as a good candidate for photodiode applications.

(Some figures in this article are in colour only in the electronic version)

## 1. Introduction

Photovoltaic properties of any heterojunction-based solar cells considerably depend on the recombination centres present in the components of the heterojunction, and especially in the presence of recombination centres at the interface of the heterojunction. These recombination centres can be due to structural defects of the crystal lattice in the vicinity of the interface or in the bulk of the junction. Detailed electrical characterization of the heterojunctions can reveal recombination centres due to different defects or impurities and potentially it can explain their influence on solar cell performance. This work aims to correlate the electrical properties of the p-ZnTe/n-CdTe heterojunction with the presence of recombination centres in the junction area.

With a direct energy band gap of 1.45 eV and a high optical absorption coefficient, CdTe is a very suitable absorber material for thin film solar cells. Thin film p-CdTe/n-CdS solar cells with a small area have shown long-term stable performance and high conversion efficiency up to 16.5% under AM1.5 illumination [1, 2]. However, the efficiencies of industrial, polycrystalline p-CdTe/n-CdS modules with large areas are still less than 10%, which indicates that improving CdTe film technology is essential [3]. An alternative approach to the enhancement of the efficiency of CdTe-based solar cells is to produce and examine other types of CdTe-based heterojunctions for photovoltaic solar energy conversion. One of the possible candidates is the p-ZnTe/n-CdTe heterojunction.

Although the gap of ZnTe (2.25 eV) is lower with respect to CdS (2.42 eV) and the fact that the diffusion

[3] Author to whom any correspondence should be addressed.

 

length of minority carriers is lower in n-CdTe (0.12–0.17 $\mu$m) with respect to p-CdTe (0.4–1.6 $\mu$m) [4–7] and the CdTe/CdS junction is much improved by a chlorine-containing atmosphere at a temperature above 673 K [4], ZnTe as a component of CdTe absorber in solar cells has an important advantage over CdS. Namely, ZnTe with the lattice parameter $a_{ZnTe} = 0.610$ nm is much better lattice matched to CdTe ($a_{CdTe} = 0.648$ nm) than CdS ($a_{CdS} = 0.583$ nm in the zinc blend crystallographic structure) [8]. In addition, CdS prefers to crystallize in the hexagonal structure with lattice parameters $a_{CdS} = 0.416$ and $c_{CdS} = 0.675$ nm [4]. Thus, one may expect that a ZnTe/CdTe interface would be structurally better than the CdS/CdTe one. The better lattice match should result in a reduction in the number of recombination centres in the junction area and thus the performance of the solar cells improves. The other important difference between CdS and ZnTe as a component of CdTe is the fact that, in contrast to CdS which prefers to be n-type, ZnTe prefers to be p-type. Since CdTe could be easily doped with either donors or acceptors it could be associated with both the n-type CdS and the p-type ZnTe. This opens a possibility of employing solar cell structures with n-type CdTe absorber.

Up to now, electrical properties of the ZnTe/CdTe p–n heterojunction were studied in quasi-bulk structures fabricated either by thermal evaporation or by vapour phase epitaxy [9, 10]. The study showed that the generation-recombination current and the diffusion current are controlled by the interface states of the junction [9], which also show a pronounced photosensitivity important for photovoltaic applications [10].

The aim of this work is to study the electrical characteristics of the p-ZnTe/n-CdTe heterostructure grown by molecular beam epitaxy (MBE) on the GaAs (1 0 0) substrate. The current density–voltage ($J$–$V$) and the capacitance–voltage ($C$–$V$) characteristics at 1 MHz are analysed and interpreted to determine the possible limitations of the p-ZnTe/n-CdTe solar cell performance.

## 2. Experimental

The investigated p-ZnTe/n-CdTe heterostructure was grown by MBE in the EPI 620 system at the Institute of Physics, Polish Academy of Sciences, Poland. Ultra-pure (7N) elemental sources of Cd, Zn and Te were used to deposit n-type CdTe (absorber layer) and subsequently p-type ZnTe (window layer) on a highly conductive $n^+$-GaAs : Si (1 0 0) substrate. The 2.64 $\mu$m thick CdTe absorber layer was highly doped by iodine donors from a $ZnI_2$ source. The estimated electron concentration in the CdTe layer was $8 \times 10^{18}$ cm$^{-3}$. The 0.4 $\mu$m thick ZnTe layer was p-type doped by nitrogen acceptors from a N-plasma source. The estimated hole concentration in the ZnTe topmost layer was $7 \times 10^{18}$ cm$^{-3}$. The thicknesses of the CdTe and ZnTe layers were determined *in situ* by reflection high-energy electron diffraction (RHEED) oscillations and measured *ex situ* by using the F10-VC-EXR (Filmetrics, Inc., San Diego, CA, USA) optical meter and the F10-VC-EXR software.

In order to measure the electrical properties of the p-ZnTe/n-CdTe devices, electrical contacts to the heterostructures were made. The contact to the top layer p-ZnTe was provided by a thermal deposition of a thin Au layer in a mesh configuration. The back contact electrode was made through the $n^+$-GaAs substrate by soldering pure indium. A silver wire was mechanically attached to the electrodes by using thermosetting silver paint. The current flow through the sample was determined using a stabilized power supply and a high-impedance Keithley 617 electrometer. Preliminary electrical characterization of the device was carried out in the temperature range 300–400 K. Current density–voltage ($J$–$V$) characteristics were measured under dark and illumination conditions. The temperature was measured by a chromel–alumel thermocouple connected to a hand held thermometer. Capacitance–voltage measurements were performed at a frequency of 1 MHz using a computerized capacitance–voltage system consisting of 410 $C$–$V$ meter interfaced via model 4108 $C$–$V$ interface under dark condition. A high-power halogen lamp containing iodine vapour and tungsten filament was used for the illumination of the studied device. The light intensity was varied by changing the distance between the device and the halogen lamp or by adjusting the input power of the lamp and it was determined by using a solar power meter (BTU-Solar Power Meter-TM-206). The schematic diagram of the p-ZnTe/n-CdTe heterojunction under illumination is shown in figure 1.

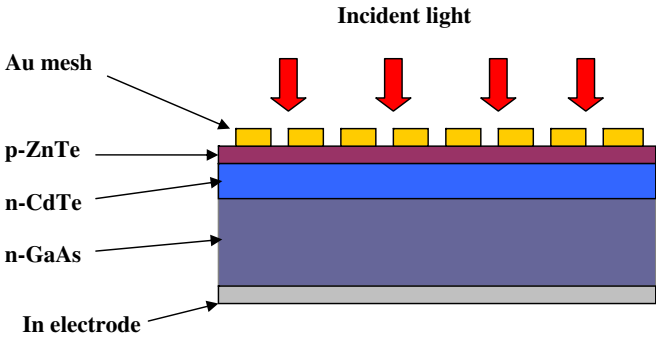


**Figure 1.** Schematic diagram of ZnTe/CdTe/GaAs heterojunction device.

## 3. Results and discussion

### *3.1. Temperature dependence of the capacitance–voltage characteristics*

The dark capacitance–voltage $C$–$V$ characteristics of the ZnTe/CdTe p–n heterojunction measured in the temperature range 300–400 K are shown in figure 2($a$). At a constant temperature, the junction capacitance significantly decreases with an increase in the reverse bias voltage. At higher temperatures, the capacitance of the diode increases. As shown in figure 2($b$), the $C$–$V$ characteristics at all temperatures can be described by the following formula [11, 12]:

$$\frac{1}{C^3} = \frac{12}{q\delta(\varepsilon_s\varepsilon_o)^2}(V_r + V_b), \qquad (1)$$

where $C$ is the junction capacitance, $\delta$ is the impurity gradient of the linearly graded junction, $\varepsilon_s\varepsilon_o$ is the permittivity of the

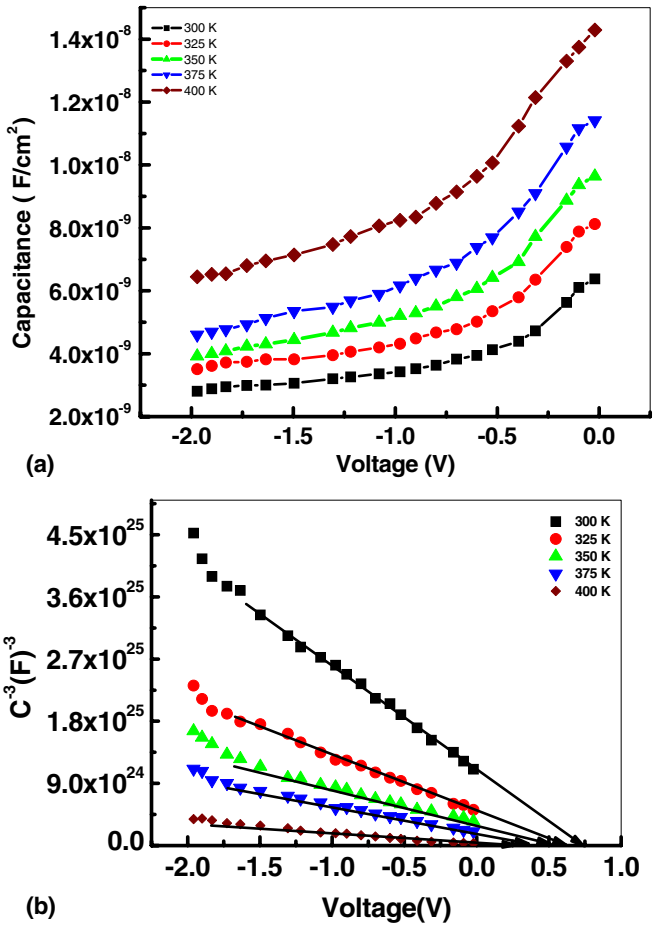


**Figure 2.** (*a*) Temperature dependence of $C$–$V$ measurements under dark condition. (*b*) Plot of $1/C^3$ versus $V$ at different temperatures.

material, $V_b$ is the built-in potential and $V_r$ is the external bias in the reverse direction.

The linear dependence of $1/C^3$ versus the reverse voltage shown in figure 2(*b*) indicates that the junction is linearly graded. The intersections of the $1/C^3$–V lines with the abscissa determine the values of the built-in potential, $V_b$, at different temperatures. From the slopes of the ($1/C^3$–$V$) lines, it is possible to determine the gradient of the impurity concentration in the depletion layer. The temperature dependences of the built-in potential and the impurity gradient are shown in figure 3. These curves clearly show that the built-in potential decreases almost linearly with an increase in temperature from 0.72 eV at 300 K down to 0.25 V at 400 K, while the impurity gradient increases with an increase in temperature.

The high values of $V_b$ may be attributed to the mid-gap states that act as recombination centres. These states arise either from the fabrication process or lattice mismatch between CdTe and ZnTe [13, 14]. Other specific causes for such phenomena are the contribution of non-uniform grain sizes, film thickness variations, interfacial oxides and others [15, 16]. The increase in the impurity gradient with an increase in $T$ has been attributed to the decrease in the width of the depletion region with the temperature as listed in table 1.

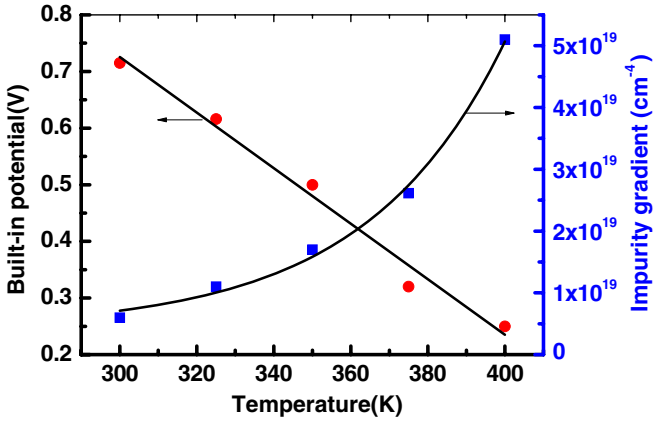


**Figure 3.** Temperature dependence of the built-in potential and the impurity gradient.

### *3.2. Temperature dependence of current–voltage characteristics*

Figure 4 shows a typical behaviour of the diode current density $J$ under forward bias voltage $V$ of the ZnTe/CdTe p–n heterojunction. The dark $J$–$V$ characteristics were taken in the temperature range 300–400 K. For the low forward bias voltage ($V < 0.35$ V), the $J$–$V$ characteristics can be described by the standard diode equation [17]:

$$J = J_o\left[\exp\left(\frac{qV}{nkT}\right) - 1\right], \tag{2}$$

where $J_o$ is the reverse saturation current density, $q$ is the electron elementary charge, $k$ is Bolzmann's constant and $n$ is the ideality factor of the junction. The first parameter determined from the data shown in figure 4 is the ideality factor, $n$, which depends on the current flow mechanism through the p–n junction. It equals 1 when the diffusion current dominates the carrier transport through the junction and becomes 2 for the generation-recombination current mechanism. The parameter $n$ can be extracted from the measured $J$–$V$ curves by using the following expression:

$$n = \frac{q}{kT}\frac{1}{\mathrm{d}\,\ln(J/J_o)/\mathrm{d}V}. \tag{3}$$

The experimental values of the ideality factor $n$ and the reverse saturation current density, $J_o$, evaluated by fitting equation (3) to the experimental $J$–$V$ characteristics are collected in table 1. The ideality factor decreases from 1.59 at 300 K down to 1.16 at 400 K, indicating that the diode current changes its character from the space-charge generation-recombination current to the diffusion current with an increase in the temperature. The generation-recombination current dominating at room temperature is a sign of a large number of defect recombination centres present in the p–n junction area. If there were no defects in the junction, the diode current would be a diffusion current and ideality factor would be equal to 1. At enhanced temperatures, the ideality factor of the device approaches 1, which shows that the width of the depletion layer is narrow and becomes comparable to the diffusion length of the

**Table 1.** The extracted parameters from $C$–$V$ and $J$–$V$ characteristics of p-ZnTe/n-CdTe device at different temperatures.

| | $T$ (K) | | | | |
|---|---|---|---|---|---|
| | 300 | 325 | 350 | 375 | 400 |
| $C_o$(F) | $5 \times 10^{-9}$ | $7 \times 10^{-9}$ | $8.3 \times 10^{-9}$ | $1.1 \times 10^{-8}$ | $1.4 \times 10^{-8}$ |
| $W$ (cm) | $2.2 \times 10^{-4}$ | $1.67 \times 10^{-4}$ | $1.35 \times 10^{-4}$ | $9.8 \times 10^{-5}$ | $7.2 \times 10^{-5}$ |
| $J_o$ (A cm$^{-2}$) | $1.75 \times 10^{-14}$ | $7.4 \times 10^{-14}$ | $7.2 \times 10^{-13}$ | $3 \times 10^{-12}$ | $7 \times 10^{-12}$ |
| $n$ | 1.59 | 1.5 | 1.39 | 1.29 | 1.16 |
| $R_s$ ($\Omega$ cm$^2$) | 499 | 455 | 386 | 355 | 292 |

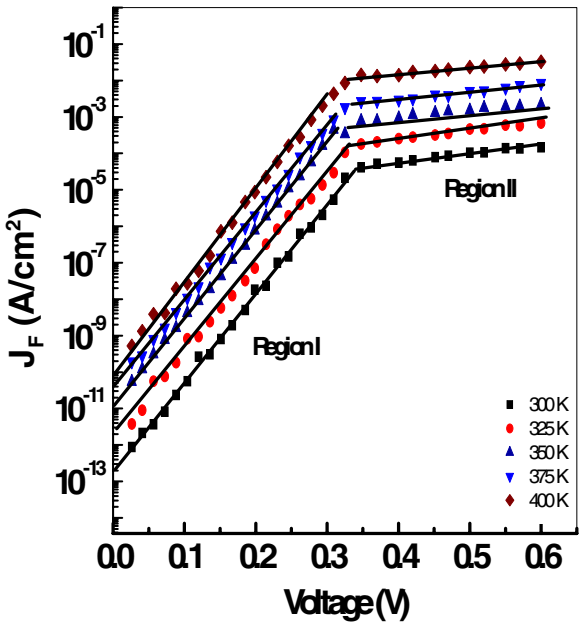


**Figure 4.** Temperature dependence of $J_F$–$V$ measurements under dark condition.

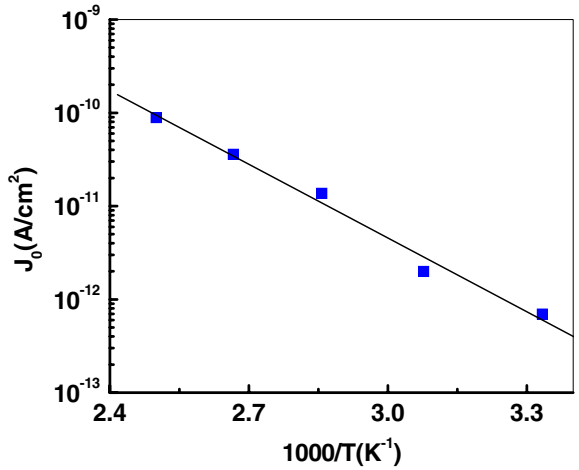


**Figure 5.** Temperature dependence of the reverse saturation current density.

carriers. The obtained results support the analysis of the $C$–$V$ characteristics.

The reverse saturation current density $J_o$ which is the second parameter determined from the data shown in figure 4, in which $J_o$ is plotted on the logarithmic scale versus the inverse temperature $T^{-1}$, is shown in figure 5. The experimental points

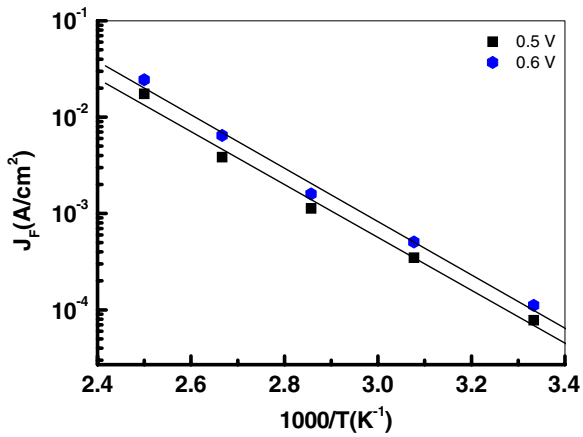


**Figure 6.** Temperature dependence of the forward current density under different biasing voltages.

follow the phenomenological expression [18]:

$$J_o = A \exp\left(\frac{-\Delta E}{kT}\right). \tag{4}$$

It is clear that the reverse saturation current is thermally activated. The estimated thermal activation energy $\Delta E$ equals 0.52 eV.

As observed from figure 4 for higher forward bias ($V > 0.35$ V), the $J$–$V$ characteristics exhibit another carrier transport mechanism. The exponential $J$–$V$ dependence is shown for the lower bias voltages changes approximately at $V = 0.35$ V but the diode current increases with increasing voltage according to a power-law dependence, $J = V^m$ with the slope $m$ of about 2. The power law of the $J$–$V$ dependence observed independently of temperature suggests that the diode current becomes space-charge-limited current (SCLC) governed by a single trap level. According to the Lampert theory, the relation for the current density in this case is given by [19–21]

$$J_{SCLC} = \frac{9}{8}\varepsilon\mu A\left(\frac{V^2}{d^3}\right)\left(\frac{N_V}{N_t(s)}\right)\exp\left(\frac{-\Delta E_t}{kT}\right), \tag{5}$$

where $d$ is the thickness of the ZnTe epilayer, $\varepsilon$ is the permittivity, $\mu$ is the hole mobility, $N_V$ is the effective density of states in the valence band edge and $N_t(s)$ is the total trap concentration at energy level $\Delta E_t$ above the valence band edge. Figure 6 shows the dependence of $J_F$ on $T^{-1}$ in the SCLC region, which yields a straight line. The slope of the straight line gives the energy of the single traps level, $\Delta E_t = 0.55$ eV.

It is interesting to note that both the reverse saturation current and the space-charge limited current are governed by single trap mechanisms with very similar activation energy. The exact nature of this trap remains unknown, but most probably it is a complex of iodine and Cd vacancy generated by the self-compensation process in highly doped n-type CdTe.

The value of series resistance $R_s$ of a solar cell is an important parameter that significantly influences the measured electrical characteristics of these devices. In general, series resistance can arise from five different sources: (1) the back contact to the semiconductor; (2) the contact made by the probe wire; (3) the resistance of the quasi-neutral bulk semiconductor at the back contact/semiconductor interface; (4) the depletion layer edge at the semiconductor surface and (5) the particular distribution interface states located at the metal/semiconductor interface. Also, the value of $R_s$ changes from region to region due to inhomogeneity of barrier height, particular distribution of interface states and surface charges [22–25].

The values of $R_s$ must be taken into account for the calculation of the main electrical parameters. There are several methods suggested in the literature [26–28] for the determination of the $R_s$ and among them the most important one is the conductance method developed by Nicollian and Brews [29]. A method to extract the $R_s$ of the ideal Schottky diodes (i.e. $n = 1$) was first proposed by Norde [27]. After that, for the $n > 1$ cases, Sato and Yasamura [24] had modified Norde's approach to extract the values of $n$, $\phi_b$ and $R_s$ from the forward bias $J$–$V$ data of the metal–semiconductor (MS) Schottky diode. Their approach requires two experimental forward bias $J$–$V$ measurements conducted at two different temperatures and the determination of the corresponding minima to the modified Norde's functions. Also Cheung and Cheung [26] presented an alternative approach to determine the values of $n$, $\phi_b$ and $R_s$ for single $J$–$V$ measurements at any temperature. When a voltage is applied across the device, the combination of the depletion layer and a series resistance of the device will share applied bias voltage and the value of $R_s$ becomes more effective especially in the accumulation region. Therefore, to achieve a better understanding of the effect of $R_s$ on the $J$–$V$ characteristics, the forward bias $J$–$V$ measurements will be taken for the ZnTe/CdTe p–n heterojunction at different temperatures.

The value of $R_s$ was calculated from the downward curvature region in the forward bias $J$–$V$ characteristics using the method of Cheung and Cheung. From equation (2), the following function can be written as

$$\frac{dV}{d\ln J} = JR_s + \left(\frac{nkT}{q}\right). \tag{6}$$

Figure 7 shows the experimental $dV/d\ln J$ versus $J$ at different temperatures for the ZnTe/CdTe heterojunction. There, the slope of this plot will give the slope $R_s$ and $nkT/q$ as the $y$-axis intercept. The obtained values of $R_s$ at different temperatures are listed in table 1. High values of $R_s$ will produce a significant reduction in the short circuit current $J_{SC}$ in these regimes, series resistance dominates and the behaviour of the solar cell resembles that of a resistor. As observed, the high values of $R_s$ are obtained which a negative effect

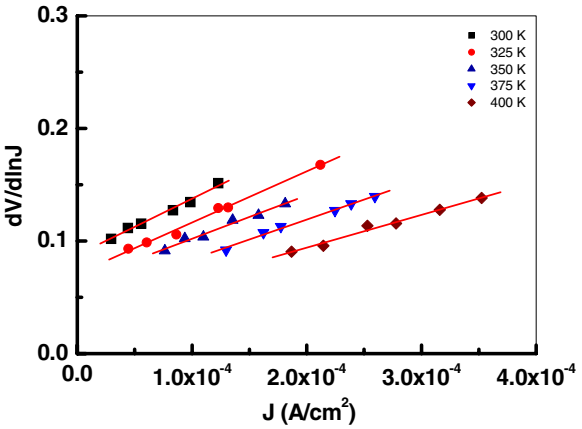


**Figure 7.** Plot of $dV/d\ln J$ versus $J$ at different temperatures.

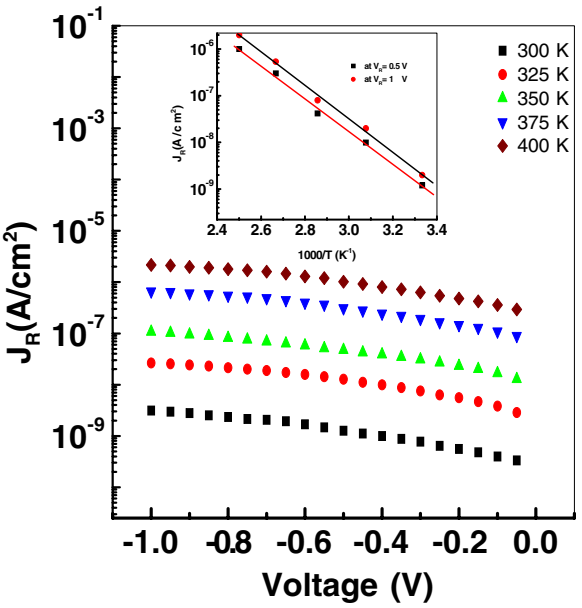


**Figure 8.** Temperature dependence of $J_R$–$V$ under dark condition. Inset: the temperature dependence of the reverse current density.

on the photocurrent has obtained from the p-ZnTe/n-CdTe heterojunction. Moreover, $R_s$ have decreased with an increase in temperature which can be attributed to the same factors responsible for the decrease in the ideality factor.

Figure 8 shows the reverse $J$–$V$ characteristics of the investigated heterojunction at various temperatures. The reverse current does not show any saturation and it is proportional to $V^{|1/2|}$ in the applied voltage range. This indicates that the dark current is governed by generation-recombination of carriers in the depletion region. The inset of figure 8 shows the temperature dependence of the reverse current of the studied heterojunction $J_R$ as a function of the inverse temperature $T^{-1}$. The Arrhenius plot appears to exhibit a thermally activated behaviour and the reverse current can be expressed as [30]

$$J_R \alpha \exp\left(\frac{-E_a}{kT}\right), \tag{7}$$

where $E_a$ is the activation energy. The activation energy calculated from the Arrhenius plot of the reverse current at 0.5 V and 1 V are 0.69 eV and 0.68 eV, respectively. These values are close to $E_g/2$ of CdTe. This confirms that the reverse current is dominated by the carrier recombination in the depletion region in the studied temperature range [11, 31].

### *3.3. Current density–voltage characteristics under illumination*

Figure 9 shows the reverse $J$–$V$ curves of the studied device under various illumination levels in the range 10–50 mW cm$^{-2}$. As observed, the photocurrent increases with reverse bias voltage and is increased by illumination. The increase in the photocurrent is due to the drift velocity of photo-generated electrons and holes in the p-ZnTe/n-CdTe interface. The photocurrent in the reverse direction is strongly increased by illumination. This behaviour yields useful information on the electron–hole pairs, which were effectively generated in the junction by incident photons. The photocurrent is higher than the dark current at the same reverse bias. This suggests that the light generates carrier-contributing photocurrent due to the production of electron–hole pairs as a result of the light absorption. The generation of photoelectrons is due to the electron transfer from n-CdTe into p-ZnTe through the potential barrier at the interface. This is a result of a difference in electron affinities between the two semiconductors. The observed strong increase in the photocurrent under the reverse bias under illumination indicates a significant photodiode sensitivity of the p-ZnTe/n-CdTe heterostructure.

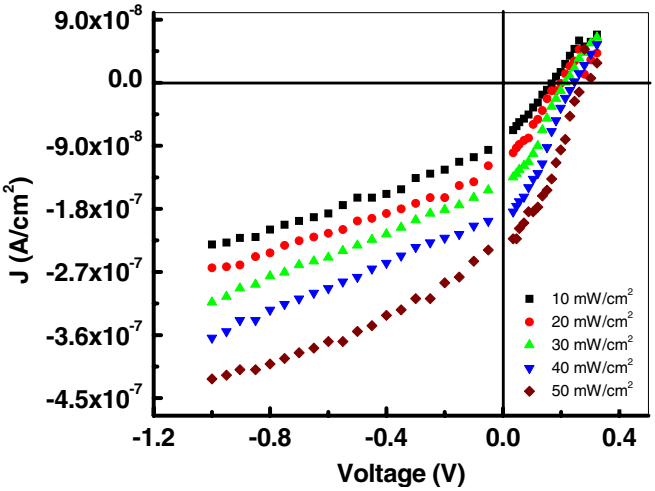


**Figure 9.** $J$–$V$ characteristics under different illumination intensities (10–50 mW cm$^{-2}$).

The photosensitivity $S$ of the p-ZnTe/n-CdTe heterojunction ($S = J_{ph}/J_{dark}$) [32] was measured under different illuminations in the range 10–50 mW cm$^{-2}$ at constant reverse bias $V_R = 0.6$ V and tabulated in table 2. These results show an increase in the phosensitivity as the illumination increases and indicate that the p-ZnTe/n-CdTe heterojunction could be used as a photodiode. The observed photocurrent-increasing phenomenon under the reverse bias indicates that the role of the depletion layer is very important. The device shows a photovoltaic behaviour with open circuit voltage $V_{oc}$ (the voltage generated by the photodiode when the photocurrent is equal to zero), and short-circuits current density $J_{sc}$ (the current per unit area flowing freely through an external circuit that has no load or resistance). The values of $V_{oc}$ and $I_{sc}$ under different illumination intensities are listed in table 2. Thus, the current in the reverse direction is strongly increased by illumination. This may be attributed to the generation of excess electron–hole pairs, which were effectively generated in the junction by incident photons.

These results suggest that the performance of a p-ZnTe/n-CdTe device can be operated as a heterojunction photodiode. In order to analyse the photoconductivity mechanism of the diodes, the variation of the photocurrent with light intensity for the designed device is shown in figure 10. The photocurrent dependence of light intensity is expressed as [33]

$$I_{ph} = BF^{\alpha}, \tag{8}$$

where $I_{ph}$ is the photocurrent, $B$ is a constant, $\alpha$ is an exponent and $F$ is the intensity of the incident light. The value of $\alpha$ for the p-ZnTe/n-CdTe heterojunction was determined from the slope of the ln $I_{ph}$ versus ln $F$ plot . We have found a value for $\alpha$ of about 0.76 at room temperature. Values of $\alpha = 0.5$ and 1.0 correspond to the bimolecular recombination and monomolecular recombination mechanism, respectively [33], whereas values for $0.5 < \alpha < 1.0$ are commonly associated with the photocarrier lifetimes determined by trapping centres. The obtained $\alpha$ value for the p-ZnTe/n-CdTe device indicates the presence of continuous distribution of traps.

## 4. Conclusion

MBE was used to grow the p-ZnTe/n-CdTe heterostructure. Capacitance–voltage and current density–voltage measurements were used to characterize the studied device. At the lower forward bias voltage, the current through the junction is limited by the generation-recombination mechanism and the built-in potential reaches 0.7 eV at 300 K. At the elevated temperatures, the junction current changes to the diffusion one and

**Table 2.** The open circuit voltage $V_{oc}$, short circuit current density $J_{sc}$ and photosensitivity $S$ of p-ZnTe/n-CdTe device at different illumination intensities.

| | $F$ (mW cm$^{-2}$) | | | | |
|---|---|---|---|---|---|
| | 10 | 20 | 30 | 40 | 50 |
| $V_{oc}$ (V) | 0.16 | 0.19 | 0.225 | 0.25 | 0.28 |
| $J_{sc}$ (A cm$^{-2}$) | $8.1 \times 10^{-8}$ | $1.1 \times 10^{-7}$ | $1.5 \times 10^{-7}$ | $1.9 \times 10^{-7}$ | $2.3 \times 10^{-7}$ |
| $S$ ($J_{ph}/J_{dark}$) | 120.7 | 138.9 | 159.1 | 188.3 | 238.9 |

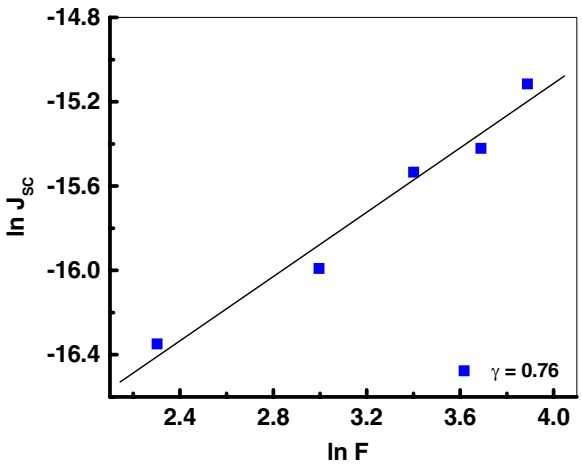


**Figure 10.** Variation of the photocurrent versus the light intensity of the p-ZnTe/n-CdTe photodiode.

the built-in potential significantly decreases. The measurements of the p-ZnTe/n-CdTe interface revealed the presence of a deep defect state with the activation energy of 0.52 eV which governs the current flow through the junction. At the higher voltage ($V > 0.35$ V), the charge transport mechanism of the device is controlled by space charge-limited current mechanism with a single trap of 0.55 eV. Under illumination of 50 mW cm$^{-2}$, the p-ZnTe/n-CdTe heterostructure shows a photovoltaic behaviour with a maximum open circuit voltage $V_{oc}$ of 0.28 V and maximum short circuit current density of $2.3 \times 10^{-7}$ A cm$^{-2}$. The $J$–$V$ measurement carried out under different illumination intensities exhibit strong dependence in the reverse direction as compared with the forward one. This behaviour suggests that the p-ZnTe/n-CdTe device can be operated as a heterojunction photodiode. The SCLC controlled by discrete distribution of traps was also confirmed from the variation of photocurrent with the intensity of light.

## Acknowledgments

One of the authors (Yahia) would like to acknowledge the partnership and ownership initiative (PAROWN) of the Egyptian Ministry of Higher Education and State for Scientific Research. Also, he would like to thank the Filmetrics company for thickness measurements of the prepared device.

## References

[1] Wu X, Keane J C, Dhere R G, DeHart C, Albin D S, Duda A, Gessert T A, Asher S, Levi D H and Sheldon P 2001 *Proc. 17th European Photovoltaic Solar Energy Conf. (Munich, Germany)* p 995
[2] Zweibel K 1992 *Int. J. Sust. Energy* **12** 285
[3] McCandless B E and Sites J R 2003 Cadmium telluride solar cells *Handbook of Photovoltaic Science and Engineering* ed A Luque and S S Hegedus (Chichester: Wiley) p 617
[4] Streetman Ben G and Banerjee Sanjay 2000 *Solid State Electronic Devices* 5th edn (Englewood Cliffs, NJ: Prentice-Hall) p 524
[5] Mandal K C, Basu S and Bose D N 1987 *J. Phys. Chem.* **91** 4011
[6] Tarricone L, Romeo N, Sberveglieri G and Mora S 1982 *Sol. Energy Mater.* **7** 343
[7] Rogers K D, Painter J D, Lane D W and Healy M 1999 *J. Electron. Mater.* **28** 112
[8] http://www.siliconfareast.com/lattice-constants/htm
[9] Rezaul Md and Khan H 1994 *J. Phys. D: Appl. Phys.* **27** 2190
[10] Gorleki P N, Demich N V, Makhnii V P and Ul'yanitskii K S 2000 *Inorg. Mater.* **36** 871
[11] Sze M 1981 *Physics of Semiconductor Devices* (New York: Wiley) p 868
[12] Neamen D A 1995 *Semiconductor Physics and Devices* (London: Irwin) p 352
[13] Kressed H and Butler J 1997 *Semiconductor Laser and Heterojunction LEDs* (London: Academic)
[14] Fonash S 1981 *Solar Cell Device Physics* (New York: Academic) p 150
[15] Mitchell K, Fahrenbruch A and Bube R 1977 *J. Appl. Phys.* **48** 4365
[16] Jeong W and Park G 2003 *Sol. Energy Mater. Sol. Cells* **75** 93
[17] Farag A A M, Yahia I S and Fadel M 2009 *Int. J. Hydrogen Energy* **34** 4906
[18] Serin T, Gürakar S, Serin N, Yıldırım N and Özyurt Kuş F 2009 *J. Phys. D: Appl. Phys.* **42** 225108
[19] Yoo J B, Fahrenbruch A L and Bube R H 1990 *J. Appl. Phys.* **68** 4694
[20] Zeyada H M, El-Nahass M M and El-Menyawy E M 2008 *Sol. Energy Mater. Sol. Cells* **92** 1586
[21] El-Nahass M M, Zeyada H M, Abd-El-Rahman K F and Darwish A A A 2007 *Sol. Energy Mater. Sol. Cells* **91** 1120
[22] De P 2006 *Microelectron. J.* **37** 786
[23] Sahingöz R, Kanbur H, Voigt M and Soykan C 2008 *Synth. Met.* **158** 727
[24] Chand S 2006 *Phys. B: Condens. Matter* **373** 284
[25] Bhattacharya D K, Mansingh A and Swarup P 1986 *Sol. Cells* **18** 153
[26] Cheung S K and Cheung N W 1986 *Appl. Phys. Lett.* **49** 85
[27] Norde H 1979 *J. Appl. Phys.* **50** 5052
[28] Sato K and Yasamura Y 1985 *J. Appl. Phys.* **58** 3656
[29] Nicollian E H and Brews J R 1982 *MOS (Metal Oxide Semiconductor) Physics and Techonology* (New York: Wiley) p 230
[30] Zemel A, Lukomsky I and Weiss E 2005 *J. Appl. Phys.* **98** 014504
[31] Farag A A M, Yahia I S and El-Metwally E G 2009 *J. Optoelectron. Adv. Mater.* **11** 204
[32] Okur S and Yakuphanoglu F 2009 *Sensors Actuators A: Phys.* **149** 241
[33] Yakuphanoglu F 2008 *Sensors Actuators A: Phys.* **141** 383